AFOSR-TR- 88-1298

THE UNIVERSITY OF NEW MEXICO
COLLEGE OF ENGINEERING

BUREAU OF ENGINEERING RESEARCH

STRUCTURE DYNAMIC THEORIES

FOR

DAMAGE DIAGNOSIS

by

Frederick D. Ju

Final Report
ME-145 (88) AFOSR-993-3

Submitted to Air Force Office of Scientific Research

October 1988

Unclassified
SECURITY CLASSIFICATION OF THIS PAGE

ADA203209

REPORT DOCUMENTATION PAGE

1a. REPORT SECURITY CLASSIFICATION: Unclassified	1b. RESTRICTIVE MARKINGS
2a. SECURITY CLASSIFICATION AUTHORITY	3. DISTRIBUTION/AVAILABILITY OF REPORT: Approved for public release Distribution unlimited
2b. DECLASSIFICATION/DOWNGRADING SCHEDULE	
4. PERFORMING ORGANIZATION REPORT NUMBER(S): ME-145(88) AFOSR-993-3	5. MONITORING ORGANIZATION REPORT NUMBER(S): AFOSR-TR- 88-1298
6a. NAME OF PERFORMING ORGANIZATION: University of New Mexico; 6b. OFFICE SYMBOL (If applicable)	7a. NAME OF MONITORING ORGANIZATION: Directorate of Aerospace Science Air Force Office of Scientific Research
6c. ADDRESS (City, State and ZIP Code): Albuquerque, NM 87131	7b. ADDRESS (City, State and ZIP Code): Bolling AFB, Washington, DC 20332
8a. NAME OF FUNDING/SPONSORING ORGANIZATION: Air Force Office of Scientific Research; 8b. OFFICE SYMBOL (If applicable): NA	9. PROCUREMENT INSTRUMENT IDENTIFICATION NUMBER: AFOSR-85-0085
8c. ADDRESS (City, State and ZIP Code): Bolling AFB, Washington, DC 20332	10. SOURCE OF FUNDING NOS. — PROGRAM ELEMENT NO.: 61102F; PROJECT NO.: 2302; TASK NO.: C2; WORK UNIT NO.:
11. TITLE (Include Security Classification): Structure Dynamic Theories for Damage Diagnosis	
12. PERSONAL AUTHOR(S): Frederick D. Ju	
13a. TYPE OF REPORT: Final; 13b. TIME COVERED: FROM 1/85 TO 6/88; 14. DATE OF REPORT (Yr., Mo., Day): October 28, 1988; 15. PAGE COUNT: 55	
16. SUPPLEMENTARY NOTATION	
17. COSATI CODES — FIELD / GROUP / SUB. GR.:	18. SUBJECT TERMS (Continue on reverse if necessary and identify by block number): Damage Diagnosis, Fracture, Reliability, Structure

19. ABSTRACT (Continue on reverse if necessary and identify by block number)

The present research aims toward developing structural theories which can be used to diagnose the fracture damage of structures and to assess the reliability of the damaged structures. It is assumed that the structures under consideration may develop damage through extreme excitations. Such damage can be defined as cracks occurred in the structures, the amount of energy dissipation, the deformation or any combination of the three. Therefore, it is important to know when damage has occurred in a structure. When it has, it is desirable to be able to locate it and estimate its extent. The principal achievements are (1) to develop theories for the reliability assessment of damageable structures and estimate the damage in a structure, and (2) to develop and improve mathematical models which simulate the behavior of damageable structures. These theories will assist the engineers to achieve a specified predictive accuracy in design, and to obtain a more realistic assessment of the existing damageable structures.

20. DISTRIBUTION/AVAILABILITY OF ABSTRACT: UNCLASSIFIED/UNLIMITED ☒ SAME AS RPT. ☐ DTIC USERS ☐	21. ABSTRACT SECURITY CLASSIFICATION: Unclassified
22a. NAME OF RESPONSIBLE INDIVIDUAL: Dr. Spencer Wu	22b. TELEPHONE NUMBER (Include Area Code): (202) 767-6962; 22c. OFFICE SYMBOL: AFOSR/NA

DD FORM 1473, 83 APR — EDITION OF 1 JAN 73 IS OBSOLETE.

Unclassified
SECURITY CLASSIFICATION OF THIS PAGE

DISCLAIMER NOTICE

THIS DOCUMENT IS BEST QUALITY PRACTICABLE. THE COPY FURNISHED TO DTIC CONTAINED A SIGNIFICANT NUMBER OF PAGES WHICH DO NOT REPRODUCE LEGIBLY.

FINAL REPORT

STRUCTURE DYNAMIC THEORIES

FOR

DAMAGE DIAGNOSIS

AFOSR-85-0085
January 1, 1985 - June 30, 1988

by

Frederick D. Ju
Mechanical Engineering Department
University of New Mexico
Albuquerque, NM 87131

submitted to

Air Force Office of Scientific Research

October 15, 1988

UNM Report No. ME-145(88) AFOSR-993-3

1.0 OBJECTIVE:

The present research aims toward developing structural theories which can be used to diagnose the fracture damage of structures and to assess the reliability of the damaged structures. Such theories, once verified experimentally, will be available for design engineers to apply to the damageable structures. It can also be the base for methodology which analytical and testing engineers can develop to diagnose and assess the reliability of the existing structures. It is assumed that the structures under consideration may develop damage through extreme excitations. Such damage can be defined as cracks occurred in the structures, the amount of energy dissipation, the deformation or any combination of the three. Therefore, it is important to know when damage has occurred in a structure. When it has, it is desirable to be able to locate it and estimate its extent.

Following the damage diagnosis, the principal components for damage assessment are (1) to develop theories for the reliability assessment of damageable structures and estimate the damage in a structure, and (2) to develop and improve mathematical models which simulate the behavior of damageable structures. These assessment theories will assist the engineers to achieve a specified predictive accuracy in design, and to obtain a more realistic assessment of the existing damageable structures.

2.0 RESEARCH PLANNING:

The research effort, sponsored by the Air Force of Scientific Research, made progress during the research years 1981-1984 toward developing a consistent structural theory in damage diagnosis and reliability assessment [1 through 16] (reference to Section 10.0, publications by the principal investigator F. D. Ju). The accomplishments are in phenomenal correlation, in structural modeling and in quantitative diagnosis of fracture damage. Deterministic analysis was the goal if possible. In real life, the excitation and even the structural characteristics can be random. Moreover, the measurements may be inadequate, inaccurate or garbled with noise. The reliability assessment will have to be probabilistic. With the establishment of a practical theory in mind, a plan for three years research was proposed in 1984 and approved beginning January 1, 1985.

2.1 Transmissibility Theory:

The transmissibility is defined as the ratio between the response and the excitation at two different stations on a structure. Cracks soften the structure and thus cause a change in transmissibility. The locations of transducers which measure the transmissibilities as well as the locations of excitation have been optimized for the necessary number of transducers and for the maximum measurement in the change of transmissibility. Damping property in the structure is included in the model. The research would propose an optimal rule to locate the response transducers and the number of measurements necessary in isolating the location of a crack damage and in assessing the intensity of the damage.

2.2 Experimental Verification of The Fracture Hinge Theory and The Modal Frequency Theory in Damage Diagnosis:

The analytical researches on the modal methods of damage diagnosis (both the modal frequency theory and the transmissibility theory) are based on the theoretical modeling of the crack with a fracture hinge by the principal investigator [1,2,3,8,9, 11]. No experiment was then available to establish and to verify its existence. This phase of research was considered most critical in the decision to continue the research. For the completion of the experimental research, the additional equipment and material supports from the Mechanical Engineering Department, UNM and the Sandia National Laboratories are gratefully acknowledged.

2.3 Uncertainty Theories:

The diagnostic theories are essentially inverse problems, for which the solution may not exist or multiple-valued. In the direct problem, the structure and the damage, the location and the extent of fracture, are given. The pre- and the post-damage structure can be analyzed for its corresponding frequency equations. The pre- and post-damage dynamic characteristics are, therefore, enumerable. However, in the inverse problem, the damage is not known a priori. The sufficiency of measurements is always an uncertainty. Furthermore, as the damage-softened structure tends to lower the modal frequencies, the neighboring modal frequencies could very well experience a cross-over. In the modal frequency theory, such cross-over cannot be ascertained. The types of uncertainties have to be address in order to caution the users of the theory and to suggest new theories to improve the accuracy in using the theory.

2.4 Probabilistic Theory of Multiple Fracture Distribution:

The damage diagnosis for a single crack has been developed successfully. However, given an external random excitation, the cracking location certainly is not a fixed pattern. The randomness of the first cracking location may be correlated to the material of the e structures and the characteristics of the external excitation. If the excitation, such as earthquake, is extreme, it is anticipated that multiple cracks will occur. The occurrence and location of the second crack may be correlated to the first crack, and so on. In the modal diagnostic theory, because the *a priori* knowledge in the number of cracks is lacking, the diagnosis is uncertain. Accordingly, it is necessary to develop the probability distribution of the cracking location. The established probability distribution of the cracking locations can help to identify multiple cracks at least in the probabilistic sense.

2.5 Modeling of Elastic-Plastic Multi-Degree-of-Freedom (MDF) System:

The research is the completion of the study beginning with the Single-Degree-of-Freedom (SDF) system [4,5,7,10,14,16]. The result establishes a model for a generic class of damaged structures. With such a nonlinear MDF stochastic model, the response of a damaged structure subjected to arbitrary random excitation can then be analyzed. The procedure of characterizing the system and its governing stochastic differential equation results in uncoupled differential equations of its mean response and its random component. The responses, their moments and crossmoments are solved for the statistical measures of the cumulative deformation and the cumulative energy of dissipation as damage assessment.

2.6 Reliability of Structures with Stiffness and Strength Degradation:

When a structure of friction materials, such as concrete, is subjected to strong random excitation, the structure may undergo inelastic deformations during certain cycles of loading with associated cyclic degradation in stiffness and strength. The prediction of reliability and assessment of damage depend upon the proper modeling of such structures, taking into consideration of the random characteristics of the material variables as well as the excitation. It has been observed experimentally in the structural degradation models that the rate of degradation may be related to the energy dissipation through the degrading restoring hysteretic loop. The randomness of the stiffness and strength degradation is estimated with the realization of the energy dissipation. The reliability, which is defined by the maximum deformation that never reaches an assumed and deterministic critical level, can then be evaluated based on the established theory. However, the statistical relation between the random stiffness degradation and the energy dissipation is an assumed probability density function since currently there is no data available.

3.0 TRANSMISSIBILITY THEORY:

The transmissibility theory uses the dynamic characteristics of the structural responses. Since the excitation may be carried out at some specific excitation frequencies or some known statistics of random excitations, the uncertainties arising through either insufficient measurements of modal frequencies or frequency cross-overs can thus be avoided. The theory is, therefore, most suitable for fracture diagnosis in complex structures. The analytical model has the fracture characteristics (e,ϑ) as parametric variables as in the modal frequency theory [18,19,30]. Hence, the general theory of circuit analogy [2,3,15] is used. The vector of modal displacements can be determined from given excitation $F(t) = F_m \exp(i\omega t)$ at a given excitation station [15] as,

$$y = C F_m e. \tag{3.1}$$

With the known set of shape functions, the displacement at any point in the pre- or post-damage structure can be computed. Appropriate locations of response transducers, placed on the structure, will yield the record of transmissibility for fracture diagnosis.

3.1 Transmissibility Measurement:

Transmissibility (T) is defined as the magnitude of the ratio of acceleration at a response station on the structure to the force applied at the excitation station on the structure; that is

$$T = |w/F|, \tag{3.2}$$

where the displacement 'w' may be complex to take into consideration of structural or viscous damping. To facilitate diagnosis,

the relative transmissibility (R_T) is introduced as follows

$$R_T = \frac{T_c - T_o}{T_o} = \frac{T_c}{T_o} - 1, \qquad (3.3)$$

where the subscripts c and o indicate with and without crack respectively. When the structure is excited with the excitation (amplitude, frequency and location) before and after a strong damage-causing excitation, the relative transmissibility becomes

$$R_T = (y_c/y_o) - 1 \qquad (3.4)$$

where y_c and y_o are the amplitudes at the same response station before and after the damage. The relative transmissibility thus ranges from -1 to ∞. The limits occur at the post- and pre-damage nodal points respectively for an undamped structure. Since structural damping, however weak, always exists, it is possible only to identify at a certain frequency a point of smallest amplitude of oscillation. A pseudo-node-point (PNP) thus defines a point of locally minimum amplitude of lateral oscillation for a specific frequency. The relative transmissibility is a function of the excitation location and frequency, the location of the response transducer and the fracture characteristics. The optimal locations of excitation and response are decided by convenience and maximum value of the relative transmissibility for as small a crack as possible.

3.2 Response Station:

The number of structural members to be instrumented for response transducer is governed by the influence range, which is defined by the proximity of a crack to a response station. A crack at a significant distance from a transducer is said to be outside of the influence range of the response station. In a frame structure, the frame cell, joined directly to an instrumented member, is called a neighboring cell. Any crack, developed in a

neighboring cell, will affect significantly the relative transmissibility of the instrumented member. The influence range, therefore, should include only the neighboring cells. The minimum number of transducers for a frame structure is accordingly

$$N = nm/2 \quad \text{for even } nm$$
$$(nm+1)/2 \quad \text{for odd } nm. \qquad (3.5)$$

Modal shape dictates the appropriate choice of transducer members. For instance, at the fundamental frequency excitation, there is no difference in choosing any wall (or column) for the response station. Hence, Fig. 3.1 illustrates a three-story four-span frame with possible locations of response transducers. Figure 2 shows the responses measured by stations (T) on members (16,21,22,24,27) respectively, for a crack on member 17. The curves in Figure 3.2 also illustrates the insensitive range of the crack position on member 17.

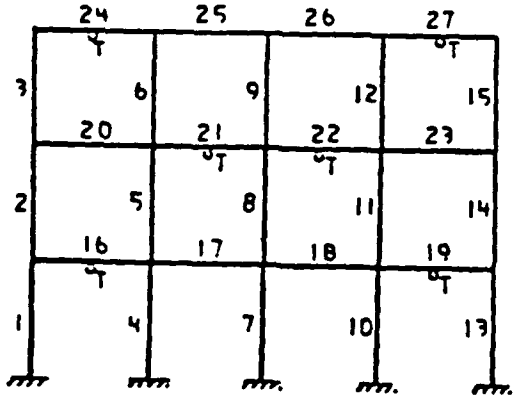

Fig. 3.1 A 3-story,4-span frame, 'T' denotes response station

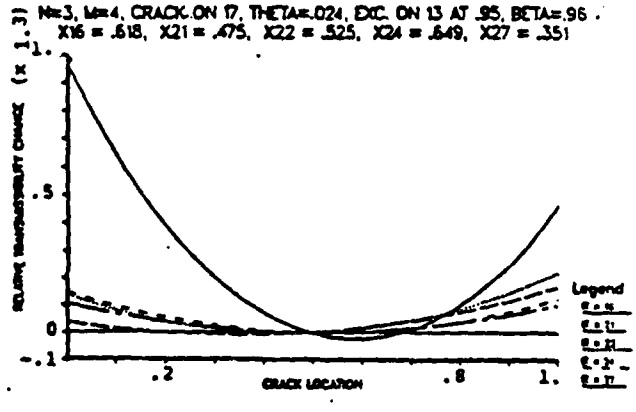

Fig. 3.2 Relative transmissibility vs. crack location (excitation on 13)

For maximum measures of relative transmissibility, it is seen that the response station should be near the pseudo-node-point. However, measurability must also be considered. In

order to avoid misreading the measurement, it is recommended that a pair of offset transducers be placed at each response station.

3.3 Damage Diagnosis:

The relative frequency measures at various response stations can be used through their influence ranges for the location of the cracked member. For instance, when the response station on member 21 records a relative transmissibility of 2.127. At such a high value, it can rest assured that the other response stations will register relative transmissibility less than 1. The cracked member is No. 21. However, if the value is 0.930, the cracked members could be No. 5, 8, 20, or 21. Member 5 could be ruled out since softening of that member would left-shift the PNP to result in most likely negative values for the relative transmissibility. For other members, the records of other response stations can help to identify the damage. For instance, an equal reading of the relative transmissibility on the response station of No. 22 implies symmetry. The cracked member is then the column No. 8. If the relative transmissibility on No. 22 response station is small, the crack will be on the beam No. 20. Yet an increase of the reading on No. 22 response station, the damaged member will again be the beam No. 21 itself with the crack at a less sensitive location. There is no deterministic location of the cracked position possible. However, the diagnostic result could bring the region of damage small enough to use some local diagnostic method. It was also shown in Fig. 3.2 that there is a range of crack locations, in which the crack damage does not produce sufficient dynamic change at a specific excitation frequency to allow efficient diagnosis. The effective ranges of a 3x4 frame structure are listed in Table 3.1 for the fundamental frequency excitation.

TABLE 3.1-Summary of the Diagnosable Regions

DND = no. of the beam element with the crack

DR = diagnosable region on the beam

RS = response station(s) exhibiting the most significant relative transmissibility change(s)

PD = total percentage of the beam length which is diagnosable

DND	DR	RS	PD(%)
1	.00 - .23 .71 - 1.0	16 16	56
2	.00 - .20 .35 - 1.0	16 16,21,24	44
3	.00 - .04 .33 - 1.0	24 24	51
4	.00 - .13 .84 - 1.0	16,21 16	49
5	.00 - .26 .30 - .37 .57 - 1.0	16 21 21,24	70
6	.00 - .14 .14 - .36 .36 - 1.0	21,24 21 24	78
7	.00 - .14 .20 - 1.0	16,19,24,27 16,19	34
8	.00 - .20 .20 - 1.0	21,22,16,19 21,22	62
9	.00 - .23 .70 - .00 .00 - 1.0	21,22 24,27 24,27,21,22	47
10	.00 - .21 .00 - .21 .24 - .70 .24 - .01 .0 - .00 .00 - 1.0	16 16 16 16 16,24,27 16	67

TABLE 3.2-Additional Diagnosable Regions at the Third Modal Frequency

DND	ADR	RS	APD(%)
1	.47 - .71	16	24
2	.00 - .47 .00 - .72 .70 - .00	16 16 16	49
3	.04 - .31	16	47
4	.13 - .20 .47 - .64	16 16	38
5	.00 - .47 .31 - .00	16 16	17
6	.00 - .41	21	15
7	.00 - .14 .03 - .20	16,19 16,19	17
8	.20 - .20 .20 - .00	16,19 21,22	11
9	.20 - .47	21,22	02
10	.23 - .26 .31 - .32 .70 - .31 .01 - .00	16 16 16 16	0

The "hole" can be filled with some higher frequency excitation. The effective ranges of the same frame from the third mode frequency excitation are listed in Table 2. Of course, the pseudo-node-points of those instrumented members for the third mode are different from those of the fundamental mode. However, a similar procedure may be taken for the placement of the corresponding transducers.

The transmissibility theory for structural fracture diagnosis avoids the multiple frequency problem that occurs for both of the last two uncertainties in the modal frequency theory to be explained in the uncertainty theory, Art. 5.0. The theory proposes the use of a single excitation frequency at both pre- and post-damage measurement of responses. The method is limited only by the number of transducers to be placed on the structure.

With the knowledge of the response-station influence range, the damaged member can be singled out. It is, however, to be pointed out that the transmissibility theory does not in itself diagnose the intensity of the fracture damage. Some combination usage of local inspection technique or even the modal frequency theory could be employed for local and intensity identification.

4.0 EXPERIMENTAL DIAGNOSIS OF FRACTURE DAMAGE:

The investigation aims to verify experimentally that the structural effect of a cracked section can be represented by an equivalent spring-loaded hinge, and to demonstrate experimentally the principle of fracture diagnosis in structures by the modal frequency theory [1,11].

4.1 The Modal Frequency Theory:

The modal frequency theory uses the structural dynamic concept that the modal frequencies change as a result of structural softening from the presence of a set of cracks of intensity $\{\gamma_k\}$, at locations, $\{e_k\}$. The fracture intensity is related through the concept of fracture hinge to the hinge spring constant κ. The softening of the structure is related to the fracture hinge spring constant and the flexibility of the structure. For each crack, it is defined by a sensitivity number ϑ. For a beam of rectangular cross-section

$$\vartheta = \frac{EI}{\kappa \ell} = 3\pi(1-\nu^2)\frac{b}{\ell}\int_0^{\gamma} \lambda[f(\lambda)]^2 d\lambda \qquad (4.1)$$

where EI is the flexural stiffness, b is the half-depth, $\gamma=a/b$ defines the crack depth and $f(\lambda)$is the dimensionless fracture stress intensity factor. The direct and the inverse problems, relating the relative modal frequency changes $\{R_i\}$ to the fracture damage characteristics $\{e_k, \vartheta_k\}$ are thus:

$$R_i = f_i(e_k, \vartheta_k) \qquad (4.2)$$

$$(e,\vartheta)_k = g_k(R_i) \qquad (4.3)$$

where $R = 1-(\bar{\omega}_i/\omega_i)$, ω_i and $\bar{\omega}_i$ are the pre- and post-damage frequencies of the i-th mode. For k-number of cracks, it is necessary to have 2k number of measures of relative frequency changes (R_i). Because of the non-linear nature of the damage functions,

usually at least one additional measure of frequency change is needed to determine one unique solution from the set of multiple solutions.

4.2 Experiment on the Validity of "Fracture Hinge" Modeling of a Cracked Section:

The experiment used twenty samples of aluminum cantilever beam with milled slits to simulate cracks of controllable configuration. There are five different single-crack locations along the beam in the length modulated dimensionless locations $\{e\}$ = $\{0.01388, 0.250, 0.51388, 0.70833, 0.79166\}$. Two crack depths (10, 20) mils correspond to $\{\gamma\}$ =$\{0.21333, 0.42666\}$, or $\{\vartheta\}$ = $\{0.006, 0.024\}$. The elastic effect at the cantilever built-in end, however small, is taken into consideration in the analytical model with an elastic torsional spring. The spring constant is determined experimentally through comparison of the experimental frequencies and theoretical ones for the undamaged beam. The elastic built-in end, therefore, can be assigned a sensitivity number ϑ_o. The cracked beam is therefore modeled by a double-hinge beam. Using Equation (4.2), the relative frequency changes can be plotted analytically as functions of the crack location for the given crack geometry. Figures 4.1 and 4.2 show respectively the Mode 1 and the Mode 2 frequency changes comparing the experimental measurements of relative frequency changes with the theoretical curves for two given crack geometries. In the figures, the solid lines represents the theoretical relative modal frequency variation, based on the average sensitivity number at the built-in end. The dash lines and data points denote the actual measured changes using individual built-in end sensitivity numbers of the samples. The accuracy is better than 0.3% for the beams with the slit closer to the built-in end. For beams with the slit closer to the free end, the errors is as high as 0.7%.

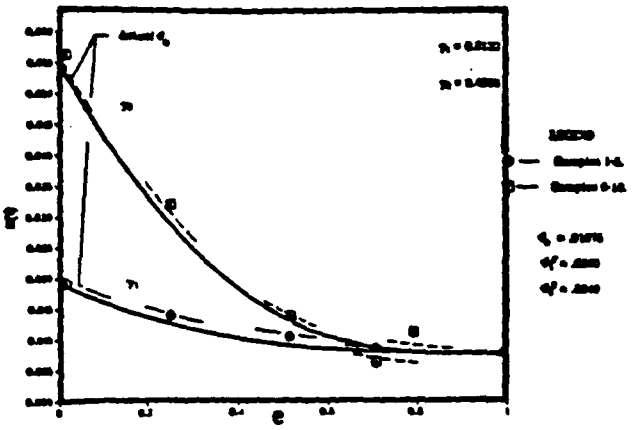

Fig.4.1 Modified Mode 1 Frequency Variations

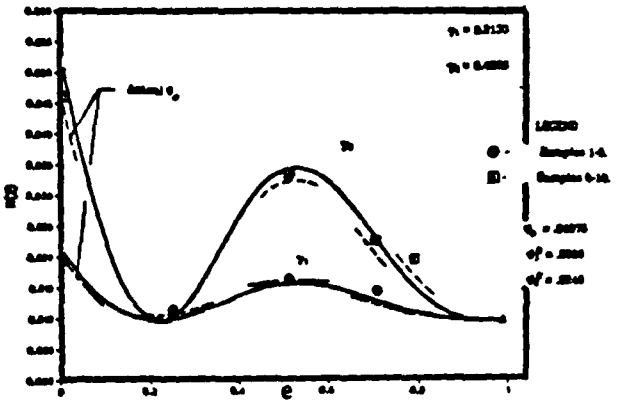

Fig.4.2 Modified Mode 2 Frequency Variation

4.3 Experimental Diagnosis of Fracture Damage:

When the built-in end sensitivity numbers of the individual sample beams are used in the double hinge model for the diagnosis of fracture damage, using the measured modal frequencies, the locations (e) of the damage intensities, in teras of individual fracture damage sensitivity numbers, are computed by the computer program FISOL, developed for the diagnostic problem [30], as listed in Table 4.1. The diagnostic solution can also be expressed in the (e,β) phase plane as shown typically in Figures 4.3 through 4.7, representing five different fracture positions. In ass five figure, solid circles denote curves for the relative frequency changes of the first mode; soled diamonds those of the second mode and solid triangles those of the third mode. The intersections of all three curves identify uniquely the solutions of the damage characteristics pairs (e,β). The diagnosed damage characteristics for the samples were compared with the actual damage characteristics of individual samples. The errors in location close to the built-in end are less than 0.05%. Up to around 1% near the free end.

TABLE 4.1

Sample No.	Relative Position θ			Sensitivity Number θ^2		
	Diagnosed	Actual	$\Delta\theta$(%)	Diagnosed	Actual	Err.(%)
1	0.014	0.01388	0.012	0.0062	0.006	3.3
2	0.241	0.250	0.9	0.0058	0.006	3.3
3	Mode-3 frequency change not measurable					
4	0.710	0.71833	0.833	0.0059	0.006	3.3
5						
6	0.0139	0.01388	0.002	0.0241	0.024	0.42
7	0.247	0.250	0.3	0.023	0.024	4.2
8	0.512	0.51388	0.19	0.024	0.024	0
9	0.7196	0.71833	0.11	0.0228	0.024	5
10	0.7802	0.79167	1.14	0.0223	0.024	7.1
11	0.0136	0.01388	0.028	0.0062	0.006	3.3
12	Mode-2 frequency change not measurable					
13	Mode-3 frequency change not measurable					
14	0.637	0.71833	8.13	0.0057	0.006	5
15	0.7974	0.79167	0.53	0.00616	0.006	2.7
16	0.0243	0.01388	0.042	0.0244	0.024	1.7
17	0.266	0.250	0.6	0.0245	0.024	2.1
18	Mode-3 frequency change not measurable					
19	0.7204	0.71833	0.207	0.0252	0.024	5
20	0.7817	0.79167	1.0	0.02453	0.024	2.2

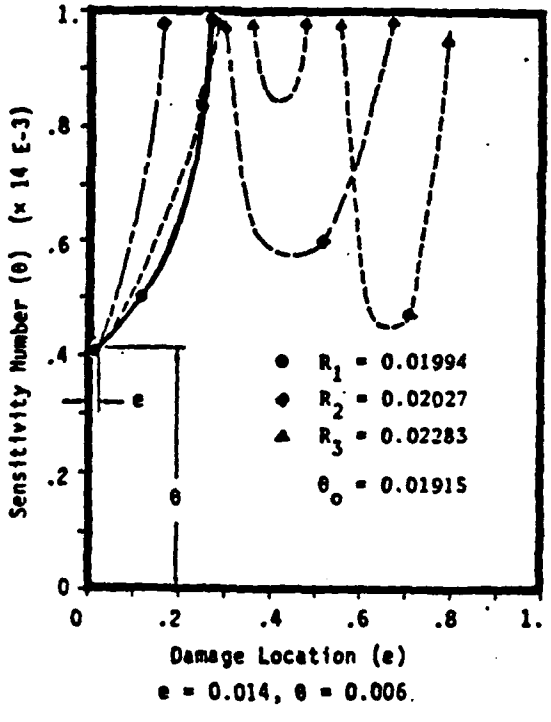

Fig.4.3 e-θ Phase Plane

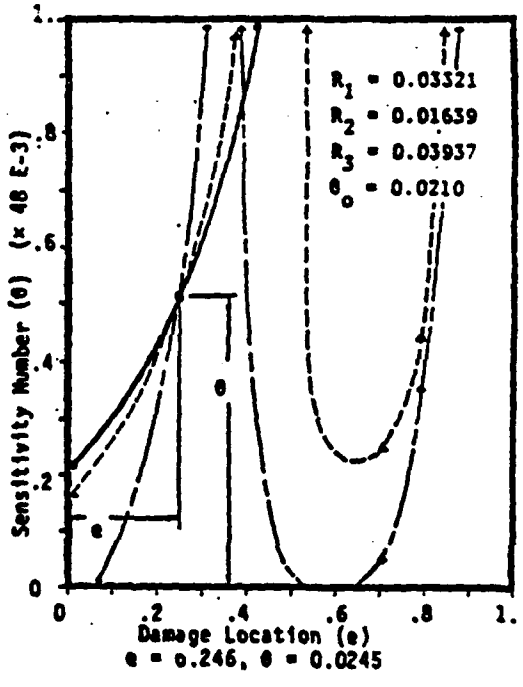

Fig.4.4 e-θ Phase Plane

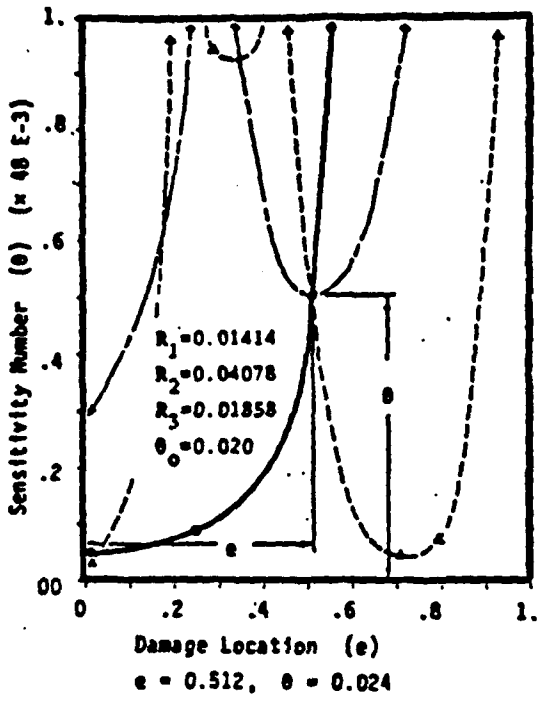

e = 0.512, θ = 0.024

Fig.4.5 e–ϑ Phase Plane

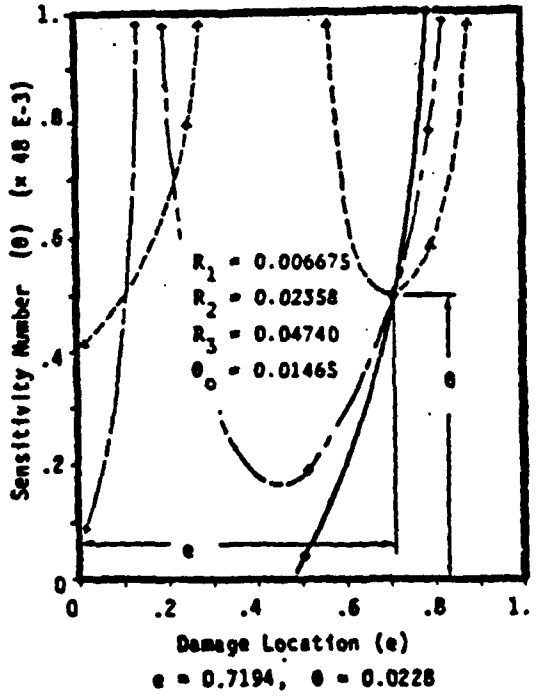

e = 0.7194, θ = 0.0228

Fig.4.6 e–ϑ Phase Plane

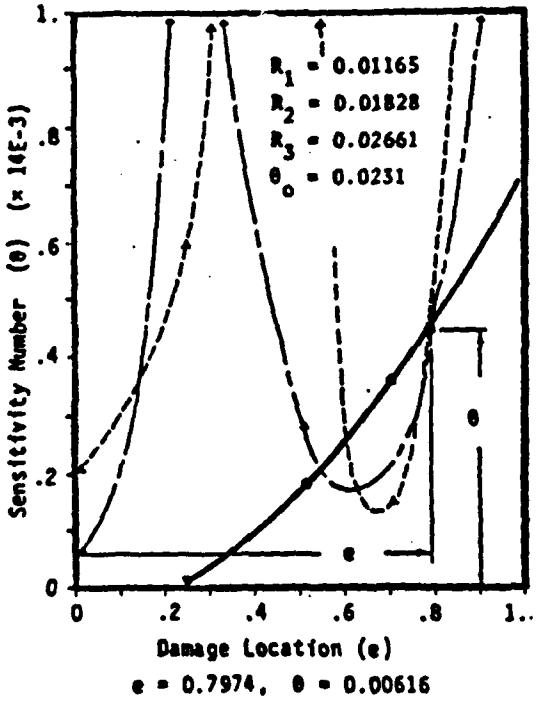

e = 0.7974, θ = 0.00616

Fig.4.7 e–ϑ Phase Plane

The research uses the experimentally obtained pre- and post-measures modal frequencies to provide a positive identification of the fracture damage [18,19,22,26,32]. The diagnostic accuracy for the two- hinge model (one hinge to simulate the elastic built-in end and another to simulate the crack) is better than 1.0% in crack locations and around 4% in damage intensities. For cracks at sections of low resisting moments, the frequency measures will be at the level of noise, resulting in large errors. Table 4.1 shows poor measurements of frequency variations for Samples Nos. 5, 10 and 14. These samples do have slits near the free end, where the moment is small. There are, however, other insufficient measurements, for which the frequency variations are in the measurement error range. As in the design of the specimens, the slits locations were designed to avoid the theoretical inflection points. However, because of the compliance of the built-in ends, slits at 0.250 and 0.51389 are in the neighborhood of mode-2 and -3 inflection points respectively. Yet, if the frequency variations in other modes are measurable, insignificant change in a particular modal frequency is an indicator that the crack may occur near that modal inflection point; while the other modal frequency variations will serve to determine the damage intensity.

5.0 UNCERTAINTY THEORY:

In the expression of the damage function, equation (4.3), it is presumed that, for k-number of cracks, (2k+1) measures of frequency changes are available for diagnosing the cracks. However, the number of cracks is generally not known a priori. Furthermore, there may not be (2k+1) measures of frequency changes available. Uncertainties thus result associated essentially with a damage configuration with multiple cracks. The lack of a priori knowledge in excitation could also lead to misinformation in modal damage, leading toward large errors in diagnosis. The investigation addresses these uncertainties.

5.1 Frequency Cross-Over:

The uncertainty of frequency cross-over can be illustrated with two modal frequencies, ω_i and ω_j (without loss of genrality let $\omega_i<\omega_j$) at undamaged state. After cracking occurs, the new modal frequencies are correspondingly $\bar{\omega}_i$ and $\bar{\omega}_j$. If the crack occurs near the inflection point of the i-th modal shape, but if the location happens to be near the maximum moment section of the j-th modal shape, $\bar{\omega}_i$ may not differ too much form ω_i. It is conceivable that, for the new modal frequencies, we may record $\bar{\omega}_j<\bar{\omega}_i$. In that case, without the knowledge of the actual damage configuration, the diagnostic assemblage of frequencies may well confuse $\bar{\omega}_j$ to be the new frequency of the i-th mode and $\bar{\omega}_i$ to be the new frequency of the j-th mode. The phenomenon is a frequency cross-over, which would commonly occur for adjacent modal frequencies of close magnitudes. The diagnostic result may be disastrous. However, with the use of transmissibility theory, for which the structure can be excited at chosen frequencies, the problem of frequency cross-over can be alleviated.

5.2 Close-Packed Multiple Cracks:

The investigation indicated that the first few characteristic values of a beam with closely spaced multiple cracks are, in general close to those of a beam with an equivalent single crack whose sensitivity number is approximately equal to the sum of the individual sensitivity numbers of the cracks on the original beam. Furthermore, the location of the equivalent crack is generally within the region where the group of cracks is located. Hence, equivalence of closely spaced cracks to a single crack implies that, in the process of damage diagnosis, it is impossible to distinguish between closely spaced multiple cracks and a single crack.[19,26,30] The limit spacing for a cantilever beam is shown in Fig. 5.1.

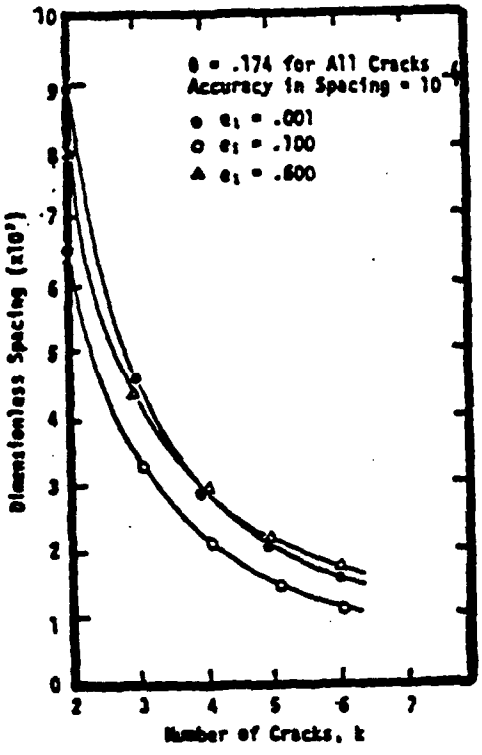

Fig. 5.1 Limit of Spacing for Multiple Cracks

5.3 Uncertainty from Inadequate Measurement:

The relative frequency changes at lower modes, for a structure with multiple cracks, may be the same or within the measurement tolerance of a structure with fewer cracks. The clarification can only be brought about with more measurements of frequency changes. Akgun and Ju [26,30] illustrated with the comparison of a single major crack against a group of ten uniformly spaced minor cracks. The first two modes yield the same frequency change. Even the third mode shows only a difference of 10^{-4}, which is, for all practical purposes, unmeasurable.

For illustration, the following relative frequency changes are assumed to have been computed from the measured frequencies of a damaged cantilever beam: R_1=.0579, R_2=.0586, R_3=.0591. It is to be determined whether the damage mainly consists of one crack. The (actual) characteristic values of a damaged beam are computed from

$$\beta_{ac}^{(j)} = \beta_u^{(j)}\sqrt{1-R_j}, \qquad (5.1)$$

where $(\beta_u^{(j)})$ are the characteristic values of the corresponding undamaged beam, the first three of which for a cantilever are (1.8751, 4.6941, 7.8548). From Equation (5.1), the third modal characteristic value of the damaged cantilever beam would be $\beta_{ac}^{(3)}$=7.6192. The first two actual characteristic values yield one solution for a single crack located at $e_{eq}^{(3)}$=.372 with γ_{eq}= 0.128 (corresponding to relative crack depth of γ=.55 for a slenderness ratio of b/L = .05). These equivalent values are then used in Equation (4.2) with k=1 to determine the third characteristic value due to the equivalent crack. The computation thus yield $\beta_{eq}^{(3)}$=7.6176. Then, the error is

$$\text{error} = (\beta_{ac}^{(3)} - \beta_{eq}^{(3)})/\beta_{ac}^{(3)} = .0002.$$

It is quite reasonable to accept a solution, whose error is less

than 0.1%. However, the given R_j data were actually generated from a problem with ten cracks of equal intensity [β was taken to be .01 (i.e., γ=.2) for all the cracks] located such that e_1=.001, e_i=.094 for i = 2,3,..,10, where e_i defines the spacing between cracks. Thus, in this case, even though the actual and equivalent $\beta^{(3)}$ values match closely, a firm diagnosis cannot be reached.

6.0 PROBABILISTIC DISTRIBUTION OF MULTIPLE CRACKS IN STRUCTURES:

The investigation considers the development of the probabilistic methodology for the prediction of multiple cracks distribution in a structure of beam elements associated with individual modal oscillations. The probabilistic measure of crack distribution can then be used for the probabilistic diagnosis of crack damage (depth) and its location (spacing) under random loading and resolve some of the intrinsic uncertainties in the modal theories of fracture diagnosis. The structural system considers some randomness of material strength. The arresting fracture toughness is characterized as a random variable with the appropriate probability distribution. The application of LEFM in connection with the stress relief effect due to the presence of crack suggests a means of predicting depth and spacing of tension cracks at a given random modal oscillation. The resulting redistributed random bending stress (moment) distribution is a measure to compute the subsequent crack state. With postulation that secondary cracking is dominantly affected by its immediately preceding crack, the process of the successive cracking can be treated as a Markov process. The analyses are performed, under these probabilistic assumptions, for the first few representative normal modes of interest. The probability distribution of the overall structural system therefore is obtained depending on weight distribution of modes for a particular excitation spectrum [28].

6.1 Crack Depth:

To estimate the depth of tension edge cracks in a beam, a fundamental fracture mechanics theory is required to assess the entire problem involved in crack initiation, propagation, and

arresting. For simplicity in the present study, only model I crack is considered to initiate if the bending stress at the extreme surface exceeds the cracking strength, σ_r. The crack propagates when the crack edge intensity factor K_I reaches a critical value K_{Ic}, fracture toughness. For crack arresting, we will assume that a crack will continue to propagate as long as K_I remains greater than some critical value K_{Io} denoted as the arresting fracture toughness. K_{Ic} may be obtained via well-defined test procedures. However, there is no test data available for K_{Io}. Since both values of K_{Ic} and K_{Io} are expected to be of the same order of magnitude, it does not seem unreasonable to treat K_{Io} as a uniform random variable in $(0,K_{Ic})$.

So long as the rate of crack growth does not approach the speed of propagation of an elastic disturbance, the computed K_I on a basis of static elastic theory should be a good approximation to describe the arresting process. Analytical solutions for K_I only exist for selected simple cases. The solution of an edge crack in half-plane is approximately applied to our beam model with edge crack length d in the presence of the bending stress field.

$$K_I = \int_0^d 1.12\sqrt{\pi d}\,\frac{2}{\pi(d^2-y^2)}\,\sigma_b(1-2y/t)dy \qquad (6.1)$$

where σ_b is the outer fibre bending stress. K_I is readily obtained by integration:

$$c(K_I/\sigma_b) = (\pi/4)\eta - \eta^3 = f(\eta), \qquad (6.2)$$

where $c = \sqrt{\pi}/t/4.48$, $\eta = d/t$, and t is the depth of the beam.

The variation of K_I with crack depth parameter η is schematically plotted in Figure 6.1, wherein $f(\eta)$ assumes its maximum value f_{max} at η_{max}. As the figures shows, if $c(K_I/\sigma_b) > f_{max}$, no crack will occur. Thus, the cracking strength σ_r can be related to K_{Ic} by applying (6.2) at η_{max}:

$$c(K_{Ic}/\sigma_r) = f_{max}, \qquad (6.3)$$

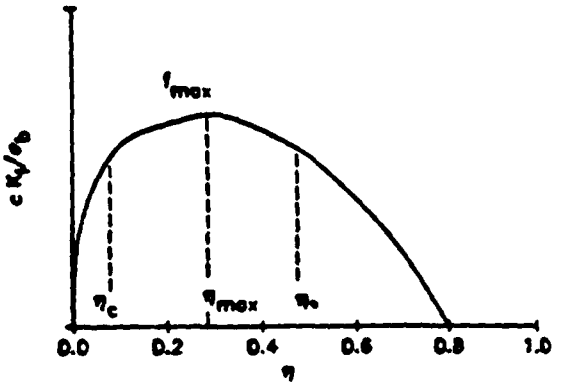

Fig. 6.1 Variation of K_I with Crack Length

which yields $\sigma_r = cK_{Ic}/f_{max}$. Equivalently, it simply says that crack occurs if $\sigma_b > \sigma_r$. Also shown in the same figure, if cK_{Io}/σ_b is less than f_{max}, there are two positive real value solutions η_c and η_o with $\eta_c < \eta_o$. η_c is interpreted as the normalized critical crack length for unstable cracking to propagate and η_o may be treated as the final crack length being arrested. Since K_{Io} is assumed to vary within $(0, K_{Ic})$, the prediction of η needs the random variable analysis. The normalized mean crack depth E[d/t] can be computed as:

$$E[d/t] = \begin{cases} 0.57(\pi/3)(\sigma_b/\sigma_r), & \sigma_b < \sigma_r \\ [0.52 - 0.15\cos(5\vartheta/3) - 0.5\cos\vartheta - 0.75\cos(\vartheta/3)](\pi/3)\cos\vartheta, & \sigma_b > \sigma_r \end{cases} \quad (6.4)$$

where $\cos\vartheta = -\sigma_r/\sigma_b$.

6.2 Crack Spacing and Stress Relief:

The quantity of principal importance to the problem of crack spacing is the stress perturbation in the plane in which cracks originate, usually the free surface. The elastic stress perturbation due to the presence of crack in the semi-infinite medium, used with the modified Griffith theory of macroscopic fracture, suggests a means of predicting spacing of tension cracks in terms of stress field and measurable properties. Since the modal theories of fracture diagnosis are non-destructive and

use low level oscillation, the measurements are carried out in the elastic range of the structure, within which the characterization of the fracture damage can be defined with LEFM. Figure 6.2 illustrates the normalized surface tangential stress relief, $g_s(\xi)$ and $g_\ell(\xi)$, respectively, for step and linear distribution of normal stresses on the crack surface. The non-dimensional variable ξ denotes the distance measure from the crack.

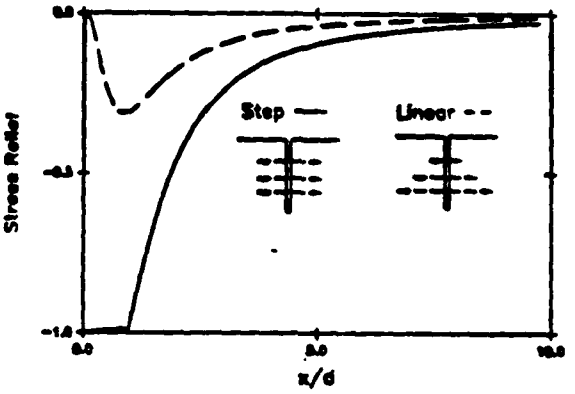

Fig.6.2 Normalized Edge Surface Bending Stress Relief

For a beam with crack depth d and the linear initial bending stress distribution across the thickness t, the bending stress relief $g(\xi)$ can be computed from the combination of $g_s(\xi)$ and $g_\ell(\xi)$ within the linear elastic range.

$$g(\xi) = g_s(\xi) - 2(d/t)\, g_\ell(\xi). \qquad (6.5)$$

6.3 The Modal Cracking Probability of Beam with Uniformly-Distributed Cracking Strength Subjected to Random Amplitude Sinusoidal Loading:

One commonly used method of numerical simulation of earthquakes is to expand a periodic function into a series of sinusoidal waves.

$$G(t) = \sum_{i=1}^{n} A_i \sin(\omega_i t + \vartheta_i), \tag{6.6}$$

where A_i is the amplitude, ω_i is the excitation frequency, and ϑ_i is the phase angle, respectively, of the i-th contributing sinusoid. Introducing randomness to ϑ_i, a wide band random excitation can be generated. In the present paper, a simple sinusoidal ground motion $G(t) = A \sin(\omega t)$ is taken with A as random variable.

For clarity convenience, the notation "(j,k) beam" is used to identify the state of a beam being in j-th mode and possessing k numbers of cracks. The associated quantities are then expressed by subscript state parameter (j,k). Thus, for a general N-crack beam system (d_{jk}, e_{jk}) is the fracture damage characteristic pair denoting the k-th crack's depth and its location at j-th mode.

The spacing s_{jk} is defined as the location difference between two sequential cracks, $e_{jk} - e_{j,k-1}$. The expression for the random edge surface stress $S_{jk}(\xi,t)$, its associated positive quantity $X_{jk}(\xi,t)$, and its related positive random quantity $Y_{jk}(\xi,t)$ beyond the random crack strength R are:

$$S_{jk}(\xi,t) = A \sin(\omega t)\varphi_{jk}(\xi), \tag{6.7}$$

$$X_{jk}(\xi,t) = S_{jk}(\xi,t)\, H[S_{jk}(\xi,t)], \tag{6.8}$$

and

$$Y_{jk}(\xi,t) = [S_{jk}(\xi,t)-R]\, H[S_{jk}(\xi,t)-R], \tag{6.9}$$

where A and R are uniformly distributed in, $(0,n\sigma_r)$ and $(0,\sigma_r)$, respectively, H is the Heavyside function, and $\varphi_{jk}(\xi)$ is the corresponding modal surface stress shape of the (j,k) beam.

6.4 Solution Procedure:

The solution of the mean time cycle of cracking, the probability of cracking, and the axial probability distribution of cracking can be formalized with procedure steps, Steps 1-3. Steps 4 and 5 compute the mean spacing between sequential cracks and the mean depth.

Step (1) For (j,k) beam with damage pair (d_{jk},e_{jk}), update the modal bending shape function $\varphi_{jk}(\xi)$ and obtain $S_{jk}(\xi,t)$, $X_{jk}(\xi,t)$ and $Y_{jk}(\xi,t)$ from Equations (6.7-6.9).

$$\varphi_{jk}(\xi) = \varphi_{j,k-1}(e_{jk})g_{jk}(\xi-e_{jk})+\varphi_{j,k-1}(\xi), \quad e_{jk}<\xi<1 \qquad (6,10)$$

Step (2) Under assumption 2, the mean time cycle m for the succeeding cracking and its cracking probability $F_{j,k+1}(\xi_{max},mT)$ can be evaluated in conjunction with $\lambda_{jk}(\xi_{max},t)$:

$$\lambda_{jk}(\xi_{max},t) = Pr[S_{jk}(\xi_{max},t)>R] =$$
$$+ Pr[A \sin(\omega t)\varphi_{jk}(\xi_{max},t)>R] =$$
$$= \begin{matrix} 1 - 1/(n \sin(\omega t)\varphi_{jk}(\xi_{max}), & 1<n\varphi_{jk}(\xi_{max})\sin(\omega t) \\ 0 & \text{otherwise} \end{matrix} \qquad (6.11)$$

$$m = \exp[-\int_0^T \lambda_{jk}(\xi_{max},\tau)d\tau] /$$
$$/(1 - \exp[-\int^T \lambda_{jk}(\xi_{max},\tau)d\tau]), \qquad (6.12)$$

and

$$F_{j,k+1}(\xi_{max},mT) =$$
$$= 1-\exp[-\int_0^T \lambda_{jk}(\xi_{max},t)dt]^m \qquad (6.13)$$

Step (3) With the evaluation of $< E[Y_{jk}(\xi,t)] >$, the axial probability density function $p_{j,k+1}(\xi,t)$ can be computed:

$$E[Y_{jk}(\xi,t)] = [n \sin(\omega t)\varphi_{jk}(\xi)/6- \frac{1}{2} + \frac{1}{2n \sin(\omega t)} \varphi_{jk}(\xi)], \qquad (6.14)$$

$$\langle E[Y_{jk}(\xi,t)]\rangle = \frac{1}{mT}\int_0^{mT} E[Y_{jk}(\xi,\tau)\,d\tau = \frac{1}{2}\int_0^{T} E[Y_{jk}(\xi,\tau)\,d\tau, \qquad (6.15)$$

and

$$p_{j,k+1}(\xi,mT) = \frac{\langle E[Y_{jk}(\xi,mT)]\rangle}{\int_{e_{jk}}^{1}\langle E[Y_{jk}(\xi,mT)]\rangle\,d\xi} = \frac{\langle E[Y_{jk}(\xi,T)]\rangle}{\int_{e_{jk}}^{1}\langle E[Y_{jk}(\xi,T)]\rangle\,d\xi}, \qquad (6.16)$$

where $e_{jk}<\xi<1$.

Step (4) Computations for mean spacing $s_{j,k+1}$ and crack location $e_{j,k+1}$ are:

$$s_{j,k+1} = \int_{e_{jk}}^{1}(\xi-e_{jk})p_{j,k+1}(\xi,mT)d\xi. \qquad (6.17)$$

and $e_{j,k+1} = s_{j,k+1} + e_{jk}$.

Step (5) For the (k+1)-th crack produced at $e_{j,k+1}$, the temporal mean stress $\langle E[X_{jk}(e_{j,k+1},mT)]\rangle$ up to time mT is:

$$\langle E[X_{jk}(e_{j,k+1},mT)]\rangle = \frac{1}{mT}\int_0^{mT} E[X_{jk}(e_{j,k+1},\tau)\,d\tau = \frac{1}{T}\int_0^{T}[\,X_{jk}(e_{j,k+1},\tau)\,d\tau. \qquad (6.18)$$

Replacing σb in Equation (6.4) by $\langle E[X_{jk}(e_{j,k+1},mT)]\rangle$ yields depth $d_{j,k+1}$. This new damage pair $(d_{j,k+1}, e_{j,k+1})$ defines a new crack state, namely, (j,k+1) beam. The loop completes and returns to step (1).

7.0 MODELING OF ELASTIC-PLASTIC STRUCTURES:

This investigation established a procedure for the probabilistic characterization of a damaged structure, which is modeled as a nonlinear elastic-plastic MDF system. The random excitation may be either stationary or nonstationary. The stiffness matrix is nonlinear to simulate the elastoplastic behavior of a damaged structure. The stiffness matrix is also random to characterize the material and environmental variations. The governing stochastic differential equation is resolved into one for the mean response and another for its random component. Responses, their statistical moments and cross-moments are solved with discrete-time recurrence formulations. The probability of structural damage or the structural reliability, is then estimated by the upper bound of the cumulative energy dissipation. The formalism of approach in formulating the solutions for a generic class of MDF nonlinear problems with Prandt-Reuss material permits ready adaptation to REM analysis. [17,31]

7.1 Formulation:

The governing differential equation of motion for a non-linear structural framework, modeled as a discrete MDF system, can be written as

$$m\ddot{z} + c\dot{z} + k(z)\, z = f \qquad (7.1)$$

where m, c, k(z) are the NxN mass, damping, and stiffness matrices, f is the external load vector; $z, \dot{z}, \ddot{z}$ are the displacement, velocity, and acceleration vectors of the system. In this investigation m,c are assumed to be deterministic and constant. The stiffness is represented by a matrix of random variable which may correlate to the response z(t). The quantities f, k(z), and z can be resolved as follows:

$$f = \phi + F, \quad k(z) = \lambda(\mu) + K, \quad z = \zeta + Z, \tag{7.2}$$

where ϕ, λ and ζ are mean values that

$$E[f] = \phi, \quad E[k(z)] = \lambda(\mu), \quad E[z] = \mu. \tag{7.3}$$

It is noted that, (7.2), the nonlinear properties of stiffness are assumed to be reflected by its mean component. The randomness of stiffness is represented by K which is a matrix of random variables. F is a non-stationary band-limited white noise. Also it is noted that the random quantities, F, K and Z introduced in (7.2) are all zero-mean. Substitution of (7.2) into (7.1) yields

$$m(\ddot{\mu}+\ddot{Z}) + c(\dot{\mu}+\dot{Z}) + [\lambda(\mu)+K](\mu+Z) = \phi + F. \tag{7.4}$$

Taking expectation on both sides of the above equation results in the mean values equation,

$$m\ddot{\mu} + c\dot{\mu} + \lambda(\mu)\mu = \phi - E[kz]. \tag{7.5}$$

The difference of (7.5) and (7.4) yields the equation for the random component.

$$m\ddot{Z} + c\dot{Z} + \lambda(\mu)Z = F + E[KZ] - KZ - K\mu. \tag{7.6}$$

In (7.5) and (7.6), KZ and E[KZ] being the product of two random quantities, are higher order terms. By neglecting these terms, (7.5) and (7.6) are reduced to the following expressions:

$$m\ddot{\mu} + c\dot{\mu} + R(\mu) = \phi, \tag{7.7}$$

$$m\ddot{Z} + c\dot{Z} + \lambda(\mu)Z = F - K\mu. \tag{7.8}$$

The omission of the higher order terms are postulated for the MDF systems. For SDF systems, the errors in response and its statistics resulting from omission of the higher order terms is referred to [17,31].

7.2 Nonlinear Model:

The investigation treated a generic class of elasto-plastic material that satisfies the Prandtl-Reuss relationship. For a beam with symmetric cross section, the moment for any section at location x, measured longitudinally along the beam, at pure bending, is

$$M(x) = EIy'' - E \int_{-c}^{c} \epsilon_o(x,h)\, hw(h)\, dh, \qquad (7.9)$$

where E is the Young's modulus, I is the moment of inertia of the cross section, y" is the second derivative of the deflection with respect to the coordinate x, c is the half depth of the symmetric cross section, $\epsilon_o(x,h)$ is the permanent set at locations x and h. All external load, without loss of generality, are resolved at nodal point. Hence

$$EIy' = E \int_o^x du \int_c^c \epsilon_o(u,h)hw(h)dh + \tfrac{1}{2}C_1x^2 + C_2x + C_3, \qquad (7.10)$$

$$EIy = E\int_0^x dv \int_0^v du \int_c^c \epsilon_o(u,h)hw(h)dh + \tfrac{1}{6}C_1x^3 + \tfrac{1}{2}C_2x^2 + C_3x + C_4 \qquad (7.11)$$

The constants C_i, i = 1,...,4 are prescribed from boundary conditions. The axial strain can be evaluated with an analogous approach.

$$\epsilon_a(x) = \frac{1}{EA}\left[P + E \int_c^c \epsilon_o(w,h)\, w(h)\, dh\right], \qquad (7.12)$$

where P is the axial force, L is the length of the beam, A is the cross-sectional area. The permanent sets are yet to be determined. For that purpose an iteration scheme is developed using a finite difference method that the displacement at time t_{j+1} can be evaluated from (7.7) by using the central difference method;

$$\mu_{j+1} = A_1^{-1}[2m\mu_j + A_3\mu_{j-1} + \Delta t^2[\varphi_j - R(\mu_j)], \tag{7.13}$$

where, $A_1 = \frac{1}{2} c\Delta t + m$, and $A_3 = \frac{1}{2} c\Delta t - m$. (7.14)

It is assumed that the system starts at rest.

In the iteration scheme, the neutral axis does not change throughout the computation. Because of this assumption, the permanent set will first converge, then alternate between two values. In such cases an approximation for the permanent sets can be established by averaging the two values.

Since (7.8) characterizes the random component of the structural response, the displacement response at time t_{j+1} can be solved by using central difference approximation. Namely,

$$Z_{j+1} = A_1^{-1}(A_{2j}Z_j + A_3Z_{j-1} + \Delta t^2 F_j - \Delta t^2 K\mu_j), \tag{7.15}$$

where A_1 and A_3 are given by (7.14) and

$$A_{2j} = 2m - \Delta t^2\lambda(\mu_j), \tag{7.16}$$

in which $\lambda(\mu_j)$ is the equivalent stiffness matrix at time t_j; the s-th column in $\lambda(\mu_j)$ is by definition,

$$\lambda_s(\mu_j) = \frac{\partial R(\mu_j)}{\partial \mu_s}. \tag{7.17}$$

The response covariance matrix $E[Z_{j+1}Z_{j+1}^T]$ can then be established.

7.2 Damage Diagnosis:

Structural damage resulting from low-cycle loading may use the cumulative cycle permanent set of the cyclic energy dissipation, if it is postulated that the cumulative damage is related to the energy dissipation in the system. In a small element of a beam, the energy dissipated in the system due to material nonlinearity can be expressed as

$$E_s = \Delta V\, E \int_0^{\epsilon} [\epsilon(t) - \epsilon_o(t)]\, d\epsilon. \tag{7.18}$$

The total energy dissipation for a beam due to material nonlinearity is therefore obtained by summing up all the small elements, resulting in

$$E_v = \sum_{\Delta V} E_s = \sum_{\Delta V} \Delta V\, E\, \Sigma[\epsilon(j\Delta t) - \epsilon_o(j\Delta t)][\epsilon(<j+1>\Delta t) - \epsilon(j\Delta t)] \tag{7.19}$$

where E_v is the total energy dissipated in a beam. It is noted that $\epsilon(t)$, $\epsilon_o(t)$ are obtained from (7.7) which represents the mean of the response. In this sense, the energy dissipation calculated by (7.19) can be used to represent the mean value of the energy dissipation. The result is used to predict an upper bound of the energy dissipation measure, considering Markov inequality,

$$Pr(x \geq d) \leq \frac{E[x]}{d} \tag{7.20}$$

where d is a positive constant. If total energy dissipation is a maximum damage criterion, the probability of damage is therefore defined by (7.20) with d representing the material constant of permissible total energy dissipation. Numerical examples are referred to [17,31].

8.0 RELIABILITY OF STRUCTURES WITH STIFFNESS AND STRENGTH DEGRADATION:

When a structure of frictional materials, such as reinforced concrete, is subjected to strong random excitations, the structure may undergo inelastic deformations during certain cycles of loading, with associated cyclic degradation in stiffness or strength, or both. The exact nature of system degradation is a function of the structural materials and the configuration, and may vary considerably from structure to structure. Basically, the deteriorated phenomenon is due to the extension of crack in the concrete, bond deterioration, bar slippage, shear deformation, and inelastic deformation of reinforcement. The most important factor is the opening and closing of the crack in the structure that alternate between compression and tension during the response cycle. Thus, the opening and closing of these cracks may eventually lead to a deteriorated stiffness and strength. As a consequence, energy is dissipated through the degradated hysteresis. It has been experimentally verified by Ju et al [14] that the rate of degradation is related to the energy dissipation through the degrading restoring hysteretic loop.

Quite frequently, the excitations of the structural system are not predictable. Examples of such loading sources are earthquake, wind, aerodynamic loads, etc. Under these types of excitations, the structural response apparently behaves randomly. The random characteristics of the loading sources together with the random system degradation lead to the desire of a coherent damage model that can be used to assess the reliability of such a system. In practice, the randomness of the excitation, together with the randomness of the system degradation, will lead to the randomness of the deteriorated restoring force to be a random process, which we refer as structural random noise. The prediction of reliability and assessment of damage depend upon the

proper modeling of such structures, taking into consideration the random characteristics of the materials as well as the excitations. Therefore, the present investigation establishes such a model that can be used to predict the liability of a generic nonlinear structural system, especially for those that show stiffness and strength degradation.

8.1 Formulation:

The nonlinear system to be considered herein is a single-degree-of-freedom (SDF) system, with the governing differential equation of motion

$$m\ddot{z} + c\dot{z} + R(z) = f(t), \tag{8.1}$$

where m,c are the mass and damping, respectively; f(t) is the external random excitation, z, $\dot{z}$, $\ddot{z}$ are the displacement, velocity and acceleration responses of the structural system, respectively. R(z) is the system hysteretic restoring force. In this investigation, m, c are assumed to be deterministic and constant. Further, it is assumed that f(t) is a band limited zero-mean stationary white noise with constant power spectral density φ_{ff}, namely,

$$E[f(t)f(s)] = \varphi_{ff}\delta(t-s). \tag{8.2}$$

The behavior of the system hysteretic restoring force for a system that shows stiffness and strength degradation has been studied extensively. Among those system-degradation hysteretic models, the Q-hysteresis can reproduce the behavior of system degradation in a simple and efficient way. Hence, it is adopted here in the present study to describe the deterministic behavior of system degradation. The rules of Q-hysteresis are summarized in Figure 8.1, in which k_1 is the initial stiffness. The unloading stiffness k_3 is determined by:

$$k_3 = k_1 [z_y/z_{max}]^{\gamma}, \qquad \gamma = 0.4. \tag{8.3}$$

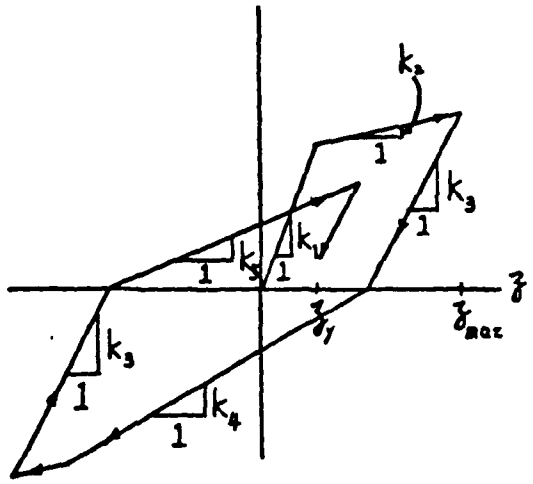

Fig. 8.1 The Q-hysteresis

It is noted that the parameters k_i, i=1,...5 in Figure 8.1 define the rules of loading, unloading and loading reversal. On a simpler level, all these parameters can be assumed that they do not manifest any randomness. However, on a more realistic level, all these parameters cannot accurately describe the original behavior of system degradation. Moreover, due to the material randomness, even two identical samples cannot yield the same hysteretic curve. Therefore, the error that between real behavior of system degradation and the model we developed, together with the random characteristics of the material, lead us to the realization that the hysteretic restoring force must behave randomly. Further, in view of the fact that the restoring force is a function of the random displacement response, the randomness of the hysteretic restoring force must be time dependent. Without loss of generality, the hysteretic restoring force can be rewritten as

$$R = R(\alpha_1,\ldots,\alpha_6) \tag{8.4}$$

where $\alpha_i = k_i$, i=1,...,5, $\alpha = z$. By using the Taylor's expansion, R can be expanded about the means of its underlying random parameters to obtain

$$R = R(\mu_1,\ldots,\mu_6) + \sum_{i=1}^{6} (\alpha_i-\mu_i)\frac{\partial R}{\partial \alpha_i} +$$

$$+ \frac{1}{2}\sum_{i=1}^{6}\sum_{j=1}^{6} (\alpha_i-\mu_i)(\alpha_j-\mu_j)\frac{\partial^2 R}{\partial\alpha_i\partial\alpha_j} + \ldots. =$$

$$= R(\mu_1,\ldots,\mu_6) + N(\xi_1,\ldots,\xi_6), \qquad (8.5)$$

where $\mu_i = E[\alpha_i]$, $\xi_i = \alpha_i-\mu_i$, $i=1,\ldots6$. It is noted that the derivatives in the above equation are evaluated at μ_i, $i=1,\ldots6$. The $N(\xi_1,\ldots,\xi_6)$ is the generalized structural noise. The structural noise arises from the uncertainty of the materials, the errors in the model and the randomness of the response. Apparently, the structural noise is a wide band random process. A typical such structural noise is shown in Figure 8.2. According to [17], the structural noise can be approximately assumed to be zero-mean with less than 1 percent error. Moreover, from Figure 8.2 it can be seen that the structural noise indeed shows the property of zero-mean. Substitution of Equation (8.5) into (8.1) yields

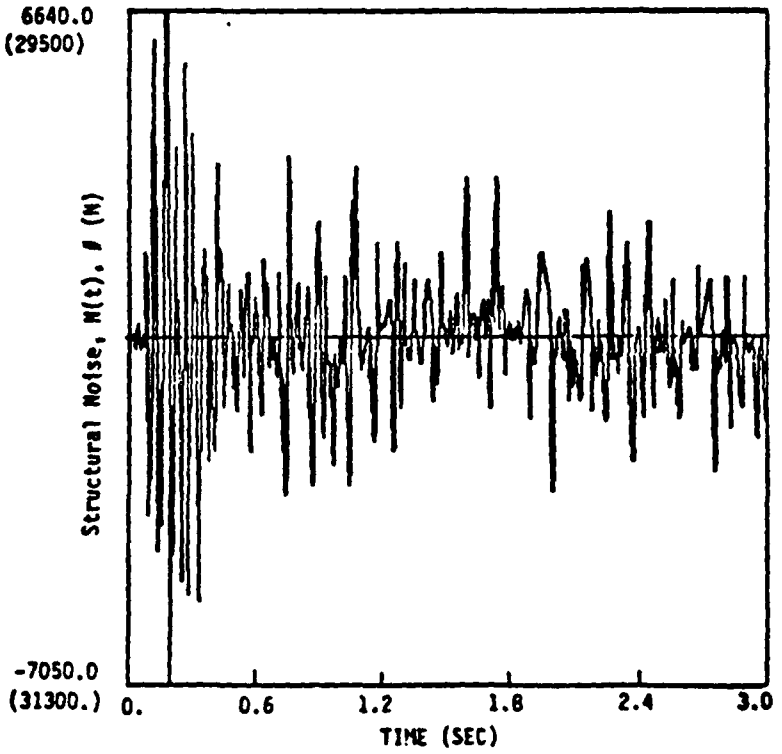

Fig. 8.2 A Typical Example of Structural Noise

$$m\ddot{z} + c\dot{z} + R(z) + N(t) = f(t). \qquad (8.6)$$

The structural noise N(t) is introduced in the above equation and is presented as a function of time for simplicity. In order to specify the characteristics of a random process, the probability structure of such a random process must be given. Namely, the probability density functions of the random process up to infinite order must be known. In practice, this is impossible. However, the difficulty is alleviated by adding more restriction when evaluating the structural noise. In the present investigation, the restriction is made by adding the energy dissipation as a given condition. In such a situation, the autocorrelation function of the structural noise can be evaluated. According to the above statements, if the wide band random noise assumption is made, the autocorrelation function can be written as

$$E[N(t)N(t+s)\,|\,E_d,\ z(t)] = S(t)\delta(s).$$

It is noted that S(t) is time dependent which reflects the nonstationary characteristics of N(t).

Furthermore, if the input excitation f(t) is assumed to a band-limited white noise, it becomes necessary that the theory of Markov process needs to be used here. In view of this, the transition probability density function is defined as

$$P \equiv P(t,\zeta,t+\Delta t,y) = P(z(t+\Delta t)=y\,|\,z(t)=\zeta,\ E_d). \qquad (8.8)$$

Equation (6) implies that the random process at time $t+\Delta t$ is evaluated with the conditions that not only $z(t)=\zeta$ has to be given, but also the energy dissipation sequence E_d must be realized. The energy dissipation sequence E_d, therefore, may be viewed as the random environment. Given different environments, the transition probability that governs the random evolution varies.Similar

to (8.8), the first and second moments of the random increments that are associated with z(t) can be defined as

$$\mu(t) = \lim_{\Delta t \to 0} \frac{1}{\Delta t} E[\Delta z \,|\, z(t)=\zeta, E_d], \tag{8.9}$$

$$\sigma^2(t) = \lim_{\Delta t \to 0} \frac{1}{\Delta t} E[\Delta z^2 \,|\, z(t)=\zeta, E_d]. \tag{8.10}$$

The Kolmogorov backward equation still holds if the derivations are followed. The reason is that the given random environments didn't change the characteristics of $\mu(t)$, $\sigma(t)$, and P. Hence, from (8.8 - 8.10), the Kolmogorov backward equation is

$$-\frac{\partial P(t,\zeta,t',y)}{\partial t'} = \mu(t) \frac{\partial P(t,\zeta,t',y)}{\partial \zeta} + \frac{\sigma^2}{2} \frac{\partial^2 P(t,\zeta,t',y)}{\partial \zeta^2} \tag{8.11}$$

where $t' = t+\Delta t$, with initial condition

$$P(t,\zeta,t',y) = \delta(\zeta-y). \tag{8.12}$$

It is reasonable to assume that P is stationary within time $[t,t']$ if Δt is small. Based upon this assumption, (8.11) becomes

$$\frac{\partial P(t,\zeta,t',y)}{\partial t} = \mu(t) \frac{\partial P(t,\zeta,t',y)}{\partial \zeta} + \frac{\sigma^2(t)}{2} \frac{\partial^2 P(t,\zeta,t',y)}{\partial \zeta^2} \tag{8.13}$$

The evaluation of $\mu(t)$ and $\sigma^2(t)$ are discussed briefly as follows. Let $\Delta z=\Delta u+\Delta Z$ where $u=E[z]$. When taking conditional expectation on Δz, from Equation (8.6) it is easy to show that

$$\mu(t) = u(t) + \frac{1}{m} E\left[\int_0^t \exp\{-\frac{\zeta}{m}(t-\tau)\} f(\tau) d\tau\right] = 0, \tag{8.14}$$

since f(t) is zero-mean, f(t) and E_d are independent. Similarly, from Equation (8.6)

$$\sigma^2(t) = \lim_{\Delta t \to 0} \frac{1}{\Delta t} E\left[c^{-2} \int_t^{t'} d\tau \int_t^{t'} d\gamma \; h(\tau)h(\gamma)\psi(t'-\tau)\psi(t'-\gamma) \,\middle|\, z(t)=\zeta, E_d)\right] \tag{8.15}$$

in which $\psi(t)=f(t)-N(t)$, $h(t)=1-\exp(-ct/m)$, where uses have been made the facts that $\Delta u=O(\Delta t)$ and $f(t)$ is zero-mean.

Equation (8.15) can be reduced further by noting the fact that $E[N(t)f(t)]=0$ since $f(t)$ is white noise [17]. The integration can be carried out to result in [21]

$$\sigma^2 = c^{-2}[\varphi_{ff}+S(t)][1-\exp(-ct/m)]^2. \qquad (8.16)$$

It is noted that $\sigma^2(t)$ is also a random variable at time t since it contains S(t). Also $\sigma^2(t)$ approaches to $c^{-2}[\varphi_{ff}+S(t)]$ as $t\to\infty$. The solution of Equation (8.13) can be solved using the Fourier transform if $\mu(t)$ and $\sigma^2(t)$ are given by (8.14 and 8.15), respectively. The solution is Gaussian distribution with parameters ζ and V; namely,

$$P(t,\zeta,t',y,S(t)) = P[z(t')=y \,|\, z(t)=\zeta, E)] =$$

$$= \frac{1}{\sqrt{2\pi V}} \exp\{-\frac{1}{2}(y-\zeta)/\sqrt{V}\} \qquad (8.17)$$

where

$$V=c^{-2}[\varphi_{ff}+S(t)]\{t+\frac{2m}{c}[1-\exp(-\frac{ct}{m})]+\frac{m}{2c}[1-\exp(-2\frac{ct}{m})]\}$$

It is noted that the transition probability given by (8.17) contains a random variable. This means that the characteristics of the transition probability is random and its value depends upon the given condition of the energy dissipation. This satisfies the original assumption which states that given different environments, the transition probability that governs the random evolution varies. The transition probability that contains random variables are called Markov chain in random environment (MCRE).

8.2 Discrete Formulation:

The transition probability established above is based on the assumption that z(t) is continuous. However, in digital computation, a discretized form is necessary. Also, the nonlinear

characteristics of R(z) and the nonstationary property of N(t) make the transition probability solved above only valid within small time intervals. Hence, these conditions necessitate the use of discretized form of (8.17). If discrete form is used, Equation (8.17) becomes

$$\{P(n,\zeta,n+1,y,S_n)\} = P_n =$$

$$= \{p(z_{n+1}=y \,|\, z_n=\zeta, z_{n-1},\ldots,z_o, E_d\} \qquad (8.18)$$

It is noted that $z_o,\ldots,z_{n-1}$ are also put into the given condition since the future may not be independent of the past for this case. The n-step transition probability is given by (8.20).

$$p^{(n)} = \{P(z_{n+1}=y \,|\, z_o, E_d)\} = P_o \prod_{j=1}^{n} P_j, \qquad (8.19)$$

where P_j, j=1,..,n are the transition probability at time step j, and P_o is the initial probability distribution of z_o. The proof of (8.19) is referred to [21].

8.3 Application:

There are two cases that can be considered here. The first case is that each of the S_n is independent. For such a case, the structural response is then a random process moving in the average environment. The mean of the n-step transition probability, in this case, is obtained by taking expectation on both sides of (8.19) yielding

$$E[P^{(n)}] = E[P_o] \prod_{j=1}^{n} E[P_j], \qquad (8.20)$$

where $E[P_j]$ is the mean transition probability at time j. This is a special case of MCRE. It other words, z(t) is a nonstationary Markov chain with one step transition probability $E[P_j]$.

It is very interesting to note that $E[P(n,\ell,n+1,y,S_n)]$ is still a valid representation of a probability density function, where $P(n,\ell,n+1,y,S_n)]$ is given by (8.18). The reason can be seen by noting that

$$E[\int_y P(n,\ell,n+1,y,S_n)\, dy] = \int_y E[P(n,\ell,n+1,y,S_n)]dy = 1. \tag{8.21}$$

By using the definition of the expectation, (8.21) can be re-written as

$$\int_y dy \int_y P(n,\ell,n+1,y,S_n)\, P(S_n)\, dS_n =$$

$$= \int_{S_n} P(S_n)dS_n \int_y P(n,\ell,n+1,y,S_n)\, dy = 1, \tag{8.22}$$

where $P(S_n)$ is the probability density function of S_n at time step n. Equation (8.22) can be used as a tool for the numerical computation and will be discussed in Section 8.2.

The second case is that S_n, n = 1,2,... are also Markovian. In such a case, the one step transition probability which is given by (8.9). It can be rewritten by using the law of total probability.

$$P(j,\ell,j+1,y,S_j) =$$

$$= \sum_{S_j} \sum_{S_o} P^*(j,\ell,j+1,y,S_j)\, P(S_j|S_o)\, P(S_o) =$$

$$= \sum_{S_j} \sum_{S_{j-1}} \cdots \sum_{S_o} P^*(j,\ell,j+1,y,S_j) P(S_j|S_{j-1}) \cdots P(S_1|S_o) P(S_o), \tag{8.23}$$

where S_j in $P^*(j,\ell,j+1,y,S_j)$ is a given, deterministic value. If we let

$$\{P(S_i|S_{i-1})\} = \Gamma_i, \qquad i=1,..,j \tag{8.24}$$

and

$$\{P(s_o)\} = \Gamma_o, \tag{8.25}$$

then

$$P = \{P(j,\ell,j+1,y,S_j)\} = P^*(j,\ell,j+1,y,S_j) \prod_{i=1}^{j} \Gamma_i. \tag{8.26}$$

The n-step transition probability then can be evaluated based upon (8.19). Numerical examples are referred to [21].

9.0 CHARACTERIZATION OF DAMAGE USING THE CONCEPT OF STRUCTURAL POWER

This investigation aims to establish a theory, using the structural power to characterize the nonlinear structures. Since a damaged structure displays uniquely the nonlinear characteristic, the established theory shall be employed to assess and to diagnose the damaged structure and to describe the extent of damage from the standpoint of energy criterion. In addition, the established structural power can also be a material characteristic for nonlinear structures. Such characteristic is important for identification of nonlinear structure as well as damage.

The fundamental purpose of structures is to protect or shield the occupants. However, while structures may be designed adequately for the anticipated excitation, many develop serious structural damage due to unexpected severe loadings or deterioration from exposure to elements. As a consequence, the structure may behave nonlinearly during excitation. Furthermore, for most cases the nonlinear behavior occurs even for undamaged status. The nonlinearity must be characterized in order to predict the structural response.

Currently, the available techniques and theories for damage diagnosis are (i) visual observation (ii) volumetric, such as X-ray, radiography and magnetic field methods, (iii) dynamic methods, such as the acoustic wave and modal theories. The first two methods, visual and volumetric, are essentially local, thus not applicable to hard-to-reach locations or to complex structures. Hence, they cannot be adapted to establish the safety and reliability of a structure for future excitation. In other words, the engineer cannot accurately estimate the reliability for the damaged structure without an analytical theory to support a reliability analysis. The dynamic theories are based upon the measurement of structural dynamics characteristics prior to and after

the damage [19], or upon the recording of structural response during a known strong excitation [13,16,17,21]. The dynamic theories are known to have uncertainties. A probabilistic theory is being developed. The strong excitation diagnostic theory depends on an accurate nonlinear system identification.

The material nonlinearity for most cases is characterized by its force deformation relationship. For example, the force-deformation hysteretic curves for elasto-plastic, work-hardening, strength degradation, or softening materials display different shapes which may be displacement dependent. If the force-deformation relationship is known precisely, it is possible that engineers can predict the structural response with good accuracy.

The problem here is that can we know precisely the nonlinear force-deformation behavior? For static case, the answer probably is positive, since the static assumption excludes the frequency dependent property. The material then may behave closely as those obtained in lab tests. However, when transient analyses are desired, many structures may or may not follow the rules which are developed in accordance with the lab test. For such a case, the difficulty is to measure the material restoring force during extreme excitation when structure behaves nonlinearly.

In many cases, it is extremely difficult to measure the structural hysteretic restoring force due to the environment restriction. As a consequence, the predicted structural response, using lab developed material model, doesn't correlated very well with the measured response, such as acceleration. The present paper, therefore, aims to establish an alternate approach to characterize the nonlinear structural behavior. The established material characteristic can be employed to define the nonlinearity of the structure during a dynamic response, to model the structural system behavior, and to predict the damage status of the structure.

9.1 Formulation of Structural Power Model:

The nonlinear system considered herein is of single-degree-of-freedom (SDF), shown in Figure 9.1, with the governing differential equation of motion

$$m\ddot{z} + c\dot{z} + R(z) = f(t), \qquad (9.1)$$

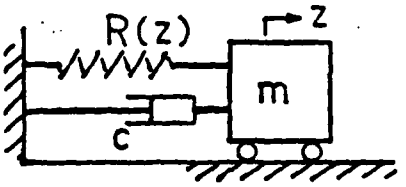

Fig. 9.1 The SDF System

where the mass (m) and the damping ratio (c) are deterministic, f(t) is the random excitation, ($\dot{z}$, $\ddot{z}$, z) are respectively the displacement, velocity and acceleration responses of the system, R(z) is the displacement-related nonlinear system hysteretic force. The hysteretic restoring force is characterized by the materials, which can be elasto-perfect plastic, work-hardening, or stiffness/strength degradation [13,17,21]. The property of stiffness/strength degradation, shown in Figure 9.2, is the typical behavior of concrete structures subject to strong excitation. As a result, the energy dissipates through the hysteretic loop. The energy dissipation (u) is thus defined as:

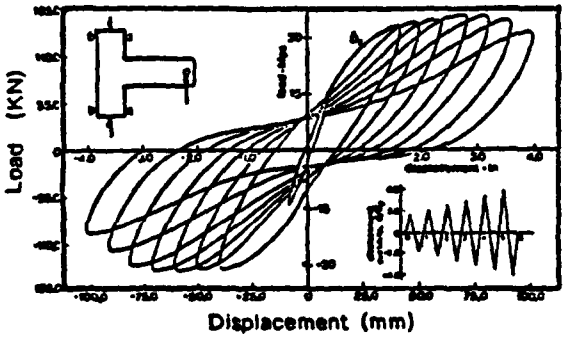

Fig. 9.2 Typical Behavior of System Degradation

$$u = \int_0^{z(t)} R(\xi)\, d\xi, \tag{9.2}$$

which represents the area under the hysteretic loop. It has been demonstrated in [13] that the amount of energy dissipation can be used as an indicator for the damage level, which is associate with the diminishing of strength and stiffness of the structure. However, currently the amount of energy dissipation is very difficult to measure, especially for a continuous structure. In view of this problem, we introduce

$$q(t) = \partial u/\partial t, \tag{9.3}$$

which represents the energy dissipation rate. Hence, the equation of motion (9.1) becomes:

$$m\ddot{z} + c\dot{z} + q(t)/\dot{z} = f(t). \tag{9.4}$$

Since q(t) represents the rate at which the energy is dissipated through the hysteretic loop, it can be viewed as a <u>structural power</u>, which is an important characteristic of a structure. If q(t) can be expressed in terms of measured responses, damage then can be identified by using q(t) as a damage indicator. Therefore, if we introduce the normalized kinetic energy (T), such that

$$T = \dot{z}^2/2, \tag{9.5}$$

the equation of motion (9.4) is thus formulated as:

$$2cT + q(t) = f(t)\,\dot{z} - m\,\partial T/\partial t. \tag{9.6}$$

The formulation (9.6) can be applied to the following problems:

(i) For an undamaged structure, the value of the structural power can be identified by computing the velocity and a controlled excitation. Such process constitutes the nonlinear system identification.

(ii) For a damaged structure, the value of the structural power will diminish as compared to that of the undamaged structure. In order to assess the extent of damage, the value of the structural power of a damaged structure must be determined. It can be done by using the process as discussed in (i).

(iii) If the velocity response is monitored during field excitation, such as earthquake, the value of the structural power can be estimated during the course of the excitation. With the estimated value of q(t), the damage status at the end of excitation can be readily enumerated.

9.2 Discussion of Structural Power:

The structural power, as defined in Sec. 2.0, is frequency dependent. To demonstrate the characteristic of frequency dependency, the Q-hysteresis model, one of the proposed models for the behavior of stiffness/strength degradation, is adopted here to simulate the structural response. The excitation illustrated first is a narrow band cosine wave random excitation:

$$f(t) = A \cos(\omega_f t + \phi), \qquad (9.7)$$

where A is the amplitude, the phase angle ϕ is a random variable with uniform distribution between 0 and 2π. When the system, as in Figure 1, with the restoring force characteristic shown in Figure 9.3, is excited by the loading given by (9.7), the energy dissipation is computed, for three different excitation frequencies — 123, 61.5, 30.75 rad/sec, Figure 9.4. The figure shows that the structural power, the slope of the energy curve, is constant for a specific narrow band random excitation.

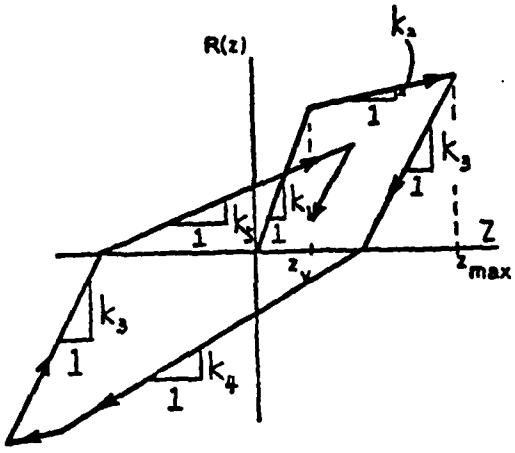

Fig. 9.3 The Q-hysteresis

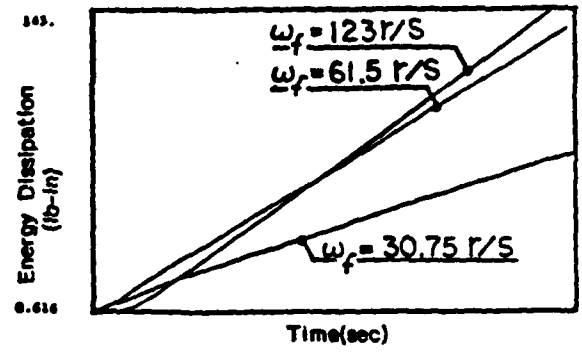

Fig.9.4 Energy Dissipation for Narrow-band Excitation

To characterize the structural power of a system subjected to wide band random excitation, the excitation will be expressed as:

$$f(t) = \sum_{i=-N}^{N} A_i \cos(\omega_i t + \vartheta_i), \qquad (9.8)$$

where A_i, i=-N,..,N, are constant, ω_i are the frequencies uniformly distributed between the frequency spectrum range (-100, 100)Hz, and the phase angles are random variables with uniform distribution between $(0,2\pi)$. With the same structural system, the normalized energy dissipation, which is defined as the energy dissipation from Q-hysteresis normalized by the quarter cycle energy dissipation at failure, was computed for 50 different excitations, given by the wide band excitation (9.8). The results are shown in Figure 9.5, from which, the structural power can be assumed as constant with the following statistics:

E[q(t)] = 0.116 j/s = constant,
Standard deviation of q = 0.011 j/s.

Furthermore, in order to illustrate the profile of the structural power vs the frequency, the same structural system is excited by the excitation as given in (9.7), with frequency ranged from

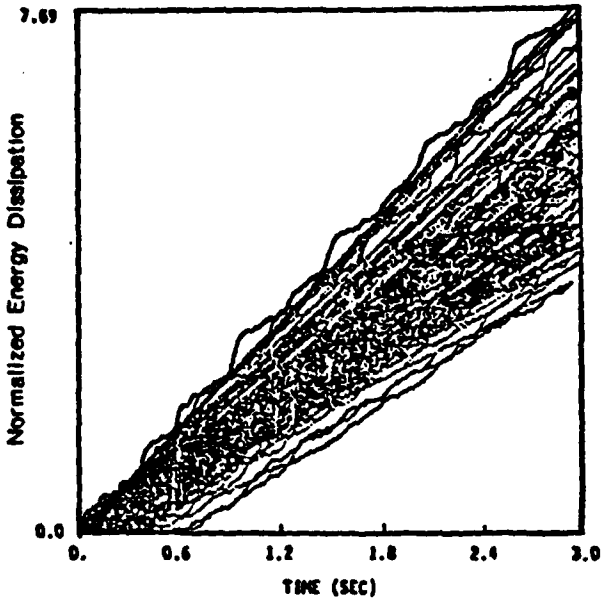

Fig.5 Energy Dissipation Sequence for wide-band Excitation

0.05 to 50 Hz. The results, shown in Figure 9.6, illustrate that the structural power (q) decreases as the excitation frequency increases. The maximum value of q occurs when the excitation frequency is in the neighborhood of the natural frequency.

Finally, in order to demonstrate the influence of the amplitude of the excitation on the structural power, the same structure system is excited by a sequence of different amplitude loadings. Figure 9.7 plots for 3 different frequencies (0.5, 1.0, 3.0 Hz) the resulting structural power vs the excitation amplitude, normalized by the yielding strength. It readily shows in Figure 9.7, that as excitation amplitude rises the value of the structural power also increases.

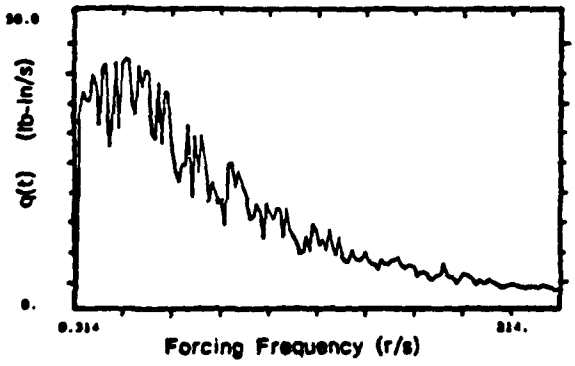

Fig.9.6 Structural Power vs Excitation frequency

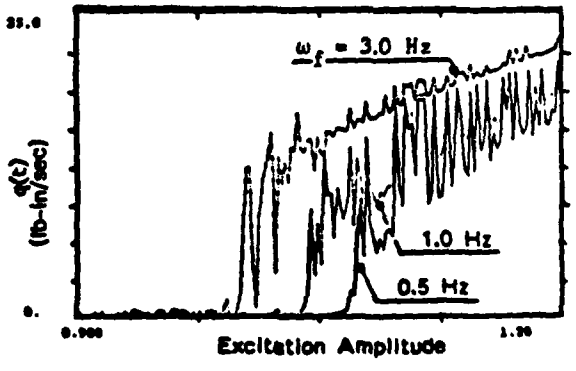

Fig.9.7 Structural Power vs Excitation Amplitude

9.3 Conclusion:

The technique of using structural power to assess the nonlinear structure requires the measurement of the structural velocity response which can be obtained by integrating the acceleration response. Therefore, it can be applied to the damage assessment conveniently. It was demonstrated that, generally, the structural power possesses a constant value for a specific excitation, either narrow or wide band. The characteristics of constant value can be further assumed as a random variable if the excitation is random. Such assumption simplifies the random analysis for structural response. The application of using structural power in random vibration analysis is discussed in [23].

10.0 PUBLICATIONS:

1. Ju, F.D., M. Akgun, E. Wang, T.L. Paez "Modal Method in Diagnosis of Fracture Damage in Simple Structures," Productive Applications of Mechanical Vibrations, ASME AMD V.52, Ed. H.C. Merchant, and T.L. Beers, Nov. 1982, pp. 113-126

2. Ju, F.D., M. Akgun and T.L. Paez "Fracture Diagnosis in Beam-Frame Structures Using Circuit Analogy," Recent Advances in Engrg. Mechanics & Their Impact on CE Practice, V.2, 1983, pp. 767-769

3. Ju, F.D., M. Akgun, T.L. Paez "Fracture Diagnosis in Structure Using Circuit Analogy," Proc. Interaction of Non-nuclear Munitions with Structures, May 1983, Colorado Springs, CO, pp. 146- 150

4. Wang, M.L., T.L. Paez, F.D. Ju "Models for Damage Diagnosis in SDF Structures," Rec. Adv. in Eng. Mech. & Their Impact of CE Practice, V.2, ASCE, 1983; Proc. Interaction of Non-nuclear Munitions with Structures, May 1983, Colorado Springs, CO, pp. 159-164

5. Wang, M.L., T.L. Paez, F.D. Ju "Identification of Inelastic MDF Systems" Engrg. Mechanics in Civil Engrg. Ed. A.P. Boresi & K.P. Chong, ASCE, Aug 1984, pp. 1005-1008

6. Paez, T.L., F.C. Chang, F.D. Ju "Least Favorable Response of Inelastic Structures," 54th Bulletin in Shock and Vibration, June 1984, pp. 143-153

7. Chang, F.C., F.D. Ju, T.L. Paez "Probabilistic Structure Dynamics of an Inelastic Structural System," Random Vibration, ASME, AMD-V. 65, Ed. T.C. Huang, Nov 1985, pp.15-23

8. Akgun, M., F.D. Ju, T.L. Paez "Transmissibility as a Means to Diagnose Damage in Structures," Proc. 3rd Internat'l Modal Anal Conf, V. II, IMAC, Union College, Schenectady, NY, Jan 1985, pp. 701-707

9. Akgun, M., F.D. Ju "Transmissibility Method in Structural Fracture Diagnosis," Proc. 2nd. Symp. on Interaction of Non-nuclear Munitions with Structures, April 1985, Panama City, FL, pp. 127-131

10. Paez, T.L., M. L. Wang, F.D. Ju "Diagnosis of Damage in SDF Structures," UNM Report No. CE-60(82)AFOSR-993-1, March 1982

11. Ju, F.D., M. Akgun, T. L. Paez, T. E. Wong "Diagnosis of Fracture Damage in Simple Structures (A Modal Method)," UNM Report No. CE-62(82) AFOSR-993-1, Nov 1982, AFOSR Technical Report AFOSR-TR-893-0049

12. Paez, T.L., F. S. Chang, F.D. Ju "Least Favorable Response of Inelastic Structures," UNM Report CE-63(83)AFOSR-993-1, March 1983

13. Wang, M.L., T.L. Paez, F.D. Ju "Mathematical Models for Damageable Structures," UNM Report CE-64(83)AFOSR-993-1, March 1983

14. Paez, T.L., M.L. Wang, F.D. Ju "Identification of Damage in Hysteretic Structures," UNM Report No. CE-78(84)AFOSR-993-1, AFOSR Technical Report AFOSR-TR-83-1230, July 1983

15. Ju, F.D., M. Akgun, T.L. Paez "A General Theory of Circuit Analogy in Fracture Diagnosis," UNM Report ME-124 (84) AFOSR-993-1, AFOSR Technical Report AFOSR-TR-84-0910, March 1984

16. Ju, F.D., T.L. Paez, F.C. Chang "Elastic-Workhardening SDF System Subjected to Random Blast Excitations," UNM Report No. ME-130(84) AFOSR Technical Report, AFOSR-993-1, Nov 1984

17. Chang, F.C., F.D. Ju, T.L. Paez "Damage Diagnosis for MDF System with Material Nonlinearity," Material Nonlinearity in Vibration Problems, ASME AMD-Vol. 71, Ed. M. Sathyamoorthy, Nov. 1985, pp. 9-19

18. Ju, F.D., M. Mimovich "Modal Frequency Method in Diagnosis of Fracture Damage in Structures," Proc. 4th Int. Modal Anal Conf., Feb. 1986, pp. 1168-1174

19. Ju, F.D. "Modal Theory of Fracture Damage Diagnosis in Structures," Role of Fracture Mech. in Modern Technology, Ed. G. C. Sih et al, Elsevier Science Pub B.V., Amsterdam, The Netherlands, 1987, pp. 589-603

20. Ju, F.D. "Modal Frequency Theory of Fracture Damage Diagnosis in Structure," Proc. Mech Failures Prevention Group, Oct 1986. (in print)

21 Chang, F.C., F.D. Ju "Reliability of Structures with Stiffness and Strength Degradation," Shock and Vibration Bulletin, No. 57, Jan. 1987, pp. 51-63

22. Ju, F.D., M. Mimovich "Experimental Diagnosis of Fracture Damage in Structures by the Modal Frequency Method" Modal Testing and Analysis, ASME DE-v.3, Ed. T.G. Carne ; J.C. Simonis, Oct 1987, pp. 29-36

23. Chang, F.C., F.D. JU "On the Correlation between Energy and Deformation," Advanced Topics in Vibration, ASME DE-vol. 8, Ed. T.C. Huang and A.V. Karvelis, Oct 1987, pp. 67-75

24. Wang, M.L., T.L. Paez, F.D. Ju "System Identification of Nonlinear Damaged Structure," Trans. SEM, Jour. Modal Analysis, v.2, No.3, 1987. pp. 128-135

25. Ju, F.D., M. Akgun "Diagnosis of Fracture Damage in Frame Structure," Trans. SEM, Jour. Modal Analysis, v.2., No.4, 1987. pp. 155-162

26. Akgun, M., F.D. Ju "Diagnosis of Multiple Cracks on a Beam Structure," Trans. SEM, Jour. Modal Analysis, v.2, No.4, 1987. pp. 149-154

27. Chang, F.C., F.D. Ju "Damage Assessment of Nonlinear Structures Using the Concept of Structural Power," Proc 6th Int Modal Anal Conf, Feb. 1988, pp. 63-66

28. Ju, F.D., Y. M. Lu "Probabilistic Distribution of Multiple Cracks in Structures due to Random Modal Oscillations," Proc 6th Int Modal Anal Conf, Feb. 1988, pp.1662-1668

29. Ju. F.D., S. L. Lu "The Reliability Assessment of Structures with Stiffness Degradation," Proc 6th Int Modal Anal Conf, Feb. 1988, pp. 250-256

30. Ju, F.D., M. Akgun "Structural Dynamic Theories of Fracture Diagnosis," UNM Report No. ME-134(85) AFOSR-993-2, January 1986

31. Ju, F.D., F.C. Chang "Damage Diagnosis for Elasto-Plastic Structures" UNM Report No. ME-138(86)AFOSR-993-2, September 1986

32. Ju, F.D., M. Mimovich "Experimental Diagnosis of Fracture Damage Using the Modal Frequency Theory" UNM Report No. ME-141(87)AFOSR -933-3, May 1987